Observation of Self-Interaction of Bernstein Waves by Nonlinear Landau Damping

Masao Sugawa
Department of Physics, Faculty of Science, Ehime University, Matsuyam, Japan
(Received 15 March 1988)

It is confirmed experimentally that the self-interaction of electron Bernstein waves occurs by means of nonlinear cyclotron (Landau) damping. This wave-particle interaction occurs in a relatively broad frequency range: $1.46 < \omega/\omega_c < 1.54$, $1.60 < \omega/\omega_c < 1.75$. The virtual wave is observed most strongly at the half-harmonic electron cyclotron frequency near $\omega/\omega_c \cong 1.5$. Although this self-interaction always occurs for $k_\parallel v_t/\omega_c \lesssim 0.1$, the virtual wave cannot be detected for $k_\parallel v_t/\omega_c \gtrsim 0.15$.

PACS numbers: 52.35.Fp, 52.35.Mw, 52.50.Gj

Recently, ion-Bernstein-wave heating at low ion cyclotron half-harmonic frequencies $\omega/\omega_{ci} \cong m/2$ has been investigated experimentally.[1-3] Also, ion heating by nonlinear absorption at $\omega/\omega_{ci} \cong \frac{3}{2}$ was investigated by Abe *et al.*,[4] on the basis of particle simulation. The possibility of bulk-ion heating by nonlinear ion cyclotron (Landau) damping has been indicated theoretically by Porkolab[5] and numerically by Sugaya[6] at $\omega/\omega_{ci} \cong \frac{3}{2}$, where the beat wave produced by the self-interaction of ion Bernstein waves resonates with the bulk ions. Furthermore, a great deal of theoretical effort has been directed to understanding the process of nonlinear Landau damping.[7-9] Experimental observations of nonlinear Landau damping have been reported for electron Bernstein waves[10] and for electrostatic waves.[11]

In this Letter observations are reported of nonlinear cyclotron (Landau) damping resulting from the self-interaction of electron Bernstein waves (hereafter referred to simply as Bernstein waves). To our knowledge, direct observation of this mechanism has not been reported previously. The resonance condition for nonlinear Landau damping in a magnetic field is given by

$$\omega - \omega'' - (k_\parallel - k_\parallel'')v_\parallel = m\omega_c, \tag{1}$$

where $(\omega,\mathbf{k})$ and $(\omega'',\mathbf{k}'')$ are the frequencies and wave vectors of the two Bernstein waves, ω_c is the electron cyclotron frequency, and m is an integer. The virtual wave $(\omega',\mathbf{k}')$ (beat wave or quasimode, $\omega'=\omega-\omega''$, $\mathbf{k}'=\mathbf{k}-\mathbf{k}''$) resonates with electrons of velocity $v_\parallel$ by means of cyclotron damping. In the case of self-interaction of Bernstein waves, $\omega''=-\omega$, $\mathbf{k}''=-\mathbf{k}$, and then $\omega'=2\omega$, $\mathbf{k}'=2\mathbf{k}$. Because Bernstein waves propagate almost perpendicularly to the magnetic field ($k_\perp \gg k_\parallel$, $|k_\parallel' v_t/\omega_c| \ll 1$), the condition $2\omega \cong m\omega_c$ is satisfied, where m is an odd integer.

Experiments were performed in a linear device[12] containing an argon plasma about 9 cm in diameter and 50 cm in length produced by a low-pressure ($\cong 2\times10^{-4}$ Torr) glow discharge in a magnetic field ($B_0=60$–100 G). The plasma parameters were as follows: density, $n_e=10^9$–10^{10} cm^{-3}, and electron temperature, $T_e=5$–7 eV. As shown in the inset of Fig. 1(a), Bernstein waves were excited by use of two antennas made of rectangular mesh plates (1.5×4.5 cm^2) (denoted by A and B); the distance between the centers of the two antennas was 4 cm. The wave propagating in the backward direction was shielded by rectangular meshes (2×5 cm^2) placed 2 mm from each antenna plate. The antenna plates were set inside about 0.5 cm from the diametrically opposed edges of the plasma column, and the antenna plane made an angle of θ ($\cong 4°$) with the magnetic field. A continuous rf signal ($P<2$ W, $\omega/2\pi=240$–300 MHz) passing through a 2ω-rejection filter was applied to A, and an rf signal with a phase difference of about 180° from A was applied to B.

Waves were detected by use of two antenna probes which were movable axially and radially. Wave patterns of waves ω were measured by means of the usual interferometer method. On the other hand, wave patterns of waves $\omega' \cong 2\omega$ across (along) the magnetic field were obtained by use of a reference signal from the axial (radial) antenna probe. Figure 1(a) shows typical wave patterns across and along the magnetic field for waves ω and $\omega' \cong 2\omega$. From curves (1) and (3), $k_\perp=8.6$ cm^{-1} and $k_\parallel=1.2$ cm^{-1} are obtained, while from curves (2) and (4), $k_\perp'=16.9$ cm^{-1} and $k_\parallel'=2.6$ cm^{-1} are obtained. Consequently $k_\parallel R \cong 0.09$ ($R=v_t/\omega_c$), and this value is determined by the distance between the exciting antennas. It is seen that $\mathbf{k}'=2\mathbf{k}$ is satisfied within the experimental error of 6%. Although the wave $(\omega',\mathbf{k}')$ is always detected for $k_\parallel R \lesssim 0.1$, we cannot detect this wave for $k_\parallel R \gtrsim 0.15$. This is ascribed to the fact that Bernstein waves are strongly damped via the interaction with resonant electrons before the occurrence of the self-interaction because the quasilinear damping rate abruptly becomes large with $k_\parallel R$. But, if a tail of higher-energy electrons exists in the distribution (which occurs mostly in a lower-pressure discharge), quasilinear damping of Bernstein waves is dominant even for $k_\parallel R \cong 0.1$. Therefore, the pressure was controlled so as to reduce tail production. Figure 1(b) shows typical frequency spectra picked up by a receiving antenna probe, where the peak at ω is heavily attenuated. The wave amplitude at ω' is as much as about 30 dB below that at ω. The waves with broad spectra ranging from 340 to 450 MHz are incoherent, and not relevant to the present experi-

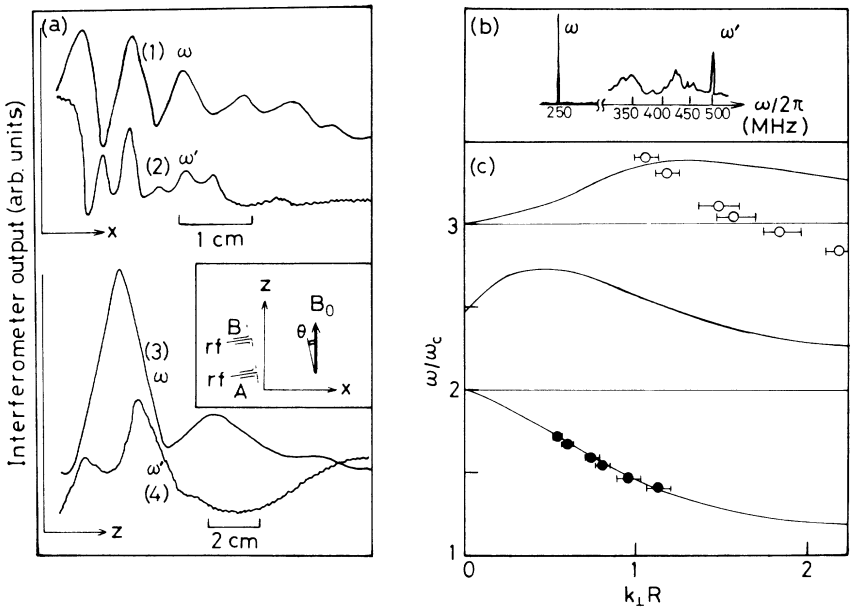

FIG. 1. (a) Interferometer output across [(1) and (2)] and along [(3) and (4)] the magnetic field for ω [(1) and (3)] and ω' [(2) and (4)]. $\omega_p^2/\omega_c^2 \cong 7.0$, $\omega/\omega_c = 1.51$, $\omega/2\pi = 250$ MHz, $\omega'/2\pi = 501$ MHz. (b) Frequency spectra of waves. (c) The ω-$k_\perp$ diagram, where filled and open circles correspond to waves ω and ω'; solid curves are the calculated dispersion relation of the Bernstein wave for $\omega_p^2/\omega_c^2 = 7.0$, $k_\parallel R = 0.09$ ($R = v_t/\omega_c$).

ment. In Fig. 1(c) the locations of frequencies and wave numbers are plotted on the calculated dispersion diagram $\epsilon = 0$, where ϵ is the dielectric function given by

$$\epsilon(\omega,\mathbf{k}) = 1 + \frac{2\omega_p^2}{k^2 v_t^2}\left[1 + \frac{\omega}{k_\parallel v_t}\sum_{n=-\infty}^{\infty}\exp(-\lambda_e) I_n(\lambda_e) Z\left(\frac{\omega - n\omega_c}{k_\parallel v_t}\right)\right]. \tag{2}$$

Here, $\lambda_e = k_\perp^2 v_t^2/2\omega_c^2$, $v_t = (2T_e/m_e)^{1/2}$, ω_p is the electron plasma frequency, I_n is the modified Bessel function of nth order, Z is the Fried-Conte plasma dispersion function, and the other notations are standard. We see that the waves $(\omega,\mathbf{k})$ fit well the dispersion of Bernstein waves. On the other hand, the waves $(\omega',\mathbf{k}')$ do not agree with the dispersion,

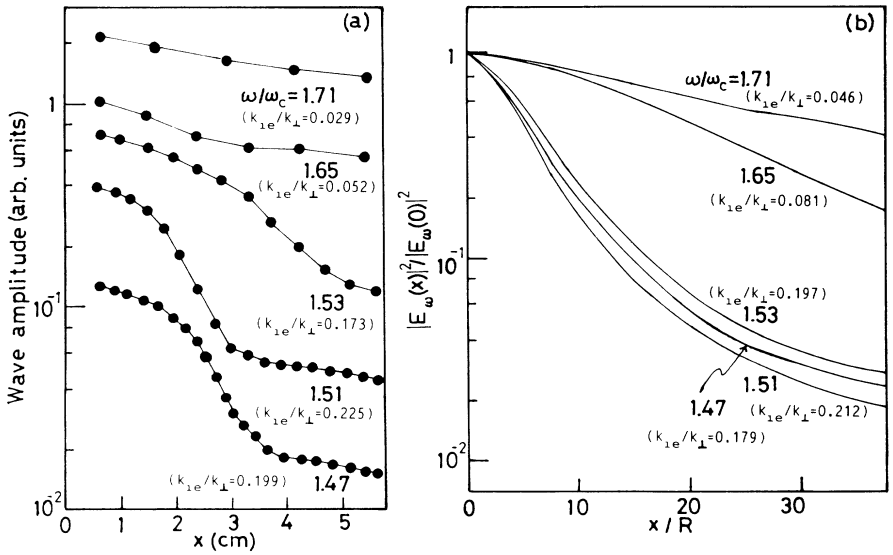

FIG. 2. (a) Spatial evolution of the amplitude of the wave $(\omega,\mathbf{k})$. (b) Calculated spatial evolution of the field energy density of the Bernstein wave, where $\omega_{p0}^2/\omega_c^2 = 9.0$, $|E_\omega|^2/16\pi n_e T_e = 0.0004$, and $k_\parallel R = 0.09$.

and their amplitudes are very weak; therefore this wave is considered to be a virtual wave (nonresonant beat wave). Figure 2(a) shows semilog plots of the wave amplitude of pump Bernstein waves versus perpendicular distance x.

The kinetic wave equation for the self-interaction of Bernstein waves by nonlinear Landau damping is[5,6,9]

$$\frac{\partial |E_\omega|^2}{\partial x} + \gamma |E_\omega|^2 = \alpha |E_\omega|^4, \tag{3}$$

where γ is the quasilinear spatial damping rate $\gamma = 2\,\mathrm{Im}(\epsilon)/[\partial\,\mathrm{Re}(\epsilon)/\partial k_\perp]$ and α is the nonlinear wave-particle coupling coefficient given by

$$\alpha = \frac{n\omega_c}{k'_\parallel v_t}\frac{\omega_p^4}{\omega_c^4}\frac{V}{4\pi^{1/2}}\frac{\exp[-(\omega'-m\omega_c)^2/k'^2_\parallel v_t^2]}{n_e T_e\,\partial\,\mathrm{Re}(\epsilon)\partial k_\perp},$$

$$V = \sum_{p,r}\frac{A - BC/D}{[(\omega/\omega_c - p)^2 - 1][(\omega/\omega_c - r)^2 - 1]}.$$

Here

$$A = \int_0^\infty d\xi (-1)^{p+r}(\partial f/\partial\xi) J_p(\rho) J_r(\rho) J_{p-m}(\rho') J_{r-m}(\rho'),$$

$$B = \int_0^\infty d\xi (-1)^{p-m}(\partial f/\partial\xi) J_p(\rho) J_m(\rho') J_{p-m}(\rho), \quad C = B(p \leftrightarrow r), \quad D = -\exp(-\lambda'_e) I_m(\lambda'_e),$$

$$f(\xi) = \exp(-\xi), \quad \xi = v_\perp^2/v_t^2, \quad \lambda_e = k'^2_\perp v_t^2/2\omega_c^2, \quad \rho = k_\perp v_\perp/\omega_c, \quad \rho' = k'_\perp v_\perp/\omega_c,$$

and J_p is the Bessel function of pth order. Also, the nonlinear equation for the virtual waves is given by

$$|E_{\omega'}|^2 = \frac{|E_\omega|^4}{|\epsilon(\omega',\mathbf{k}')|^2}\frac{\omega_p^6}{\omega_c^6}\frac{\omega_c^2}{k'^2 v_t^2}\frac{3U^2}{2\pi^3 n_e T_e}, \quad U = \sum_{p,q,r}\frac{r[(p-q)(A'+B')+rB']}{(\omega/\omega_c - q)(\omega'/\omega_c - r)}, \tag{4}$$

where $\omega' = 2\omega$, $\mathbf{k}' = 2\mathbf{k}$,

$$A' = \int_0^\infty d\xi f(\xi)(\xi/\rho'^2)(1-2\xi^2) J_{p-r}(\rho) J_q(\rho) J_r(\rho') J_{p-q}(\rho'),$$

$$B' = \int_0^\infty d\xi f(\xi)(\xi/\rho') J_{p-r}(\rho) J_q(\rho) J_r(\rho') J_{p-q}(\rho').$$

Since the wave $(\omega',\mathbf{k}')$ is the virtual wave, $\epsilon(\omega',\mathbf{k}') \neq 0$.

Figure 2(b) shows the spatial evolution of the wave amplitude calculated from the measured parameters and Eqs. (2) and (3). The spatial variation of the electron density (similar to that of the experiment) is assumed to be given by

$$\omega_p^2(X) = -0.024\omega_{p0}^2(X-5)^2 + \omega_{p0}^2, \tag{5}$$

where $X = x/(2\pi/k_\perp)$. If one compares this spatial behavior with the experimental one in Fig. 2(a), good qualitative agreement is observed. The effective damping rates (assuming exponential damping at the local position) are estimated from the curves in Figs. 2(a) and 2(b). The maximum values of these effective damping rates ($k_{ie}/k_\perp$) are given in Figs. 2(a) and 2(b). The observed values agree with the theoretical ones within a factor of 2.

In Fig. 3(a) wave patterns of the virtual wave are shown. It can be seen that virtual waves are detected in a spatially localized region, denoted by horizontal bars in Fig. 3(a). Figure 3(b) shows the spatial evolution of the virtual wave $(\omega',\mathbf{k}')$ calculated by use of Eqs. (2)–(5). The waves initially increase in amplitude, saturate, and then decrease; the position of the maximum wave amplitude varies with ω/ω_c. As shown in Figs. 3(a) and 3(b), the detectable region of the virtual waves corresponds to the region near the position of the maximum amplitude of the virtual waves obtained from the theory. Figure 3(c) shows the detectable locations of the virtual wave by vertical bars, which correspond to the horizontal bars in Fig. 3(a). The dotted curves give a contour map of the calculated equifield lines for the virtual wave. The virtual wave is not only detected for pump Bernstein waves at frequencies near half-harmonic cyclotron frequencies, but is also detected for pump waves in the frequency range $1.60 < \omega/\omega_c < 1.75$. As shown by Fig. 3(c), the appearance of virtual waves is in good qualitative agreement with the theoretical prediction. But, for pump waves in the frequency range $1.60 < \omega/\omega_c < 1.75$, the wave $(\omega',\mathbf{k}')$ may be excited because the value of $\epsilon(\omega',\mathbf{k}')$ becomes small. Therefore, one must take into account the process of resonant wave-wave interaction in this frequency range.

The existence of a threshold of the electric field energy of the pump wave for the detection of the virtual waves also was observed ($|E_\omega|^2/16\pi n_e T_e \gtrsim 5\times 10^{-5}$; this estimation has an error of a factor of 6). It seems to correspond to the theoretical threshold $|E_\omega|^2 \gtrsim \gamma/\alpha$ from Eq. (3). Further, an increase (up to 10%) of the electron temperature is observed only at detectable locations of the virtual wave.

In summary, it was confirmed experimentally that the self-interaction of the Bernstein wave occurs by means of nonlinear Landau damping. This wave-particle interaction occurs in a relatively broad frequency range, $1.46 < \omega/\omega_c < 1.54$, $1.60 < \omega/\omega_c < 1.75$. The virtual wave is observed most strongly at a frequency near $\omega/\omega_c \cong 1.5$. This self-interaction is always observed for $k_\parallel R \lesssim 0.1$ but does not occur for $k_\parallel R \gtrsim 0.15$. I believe

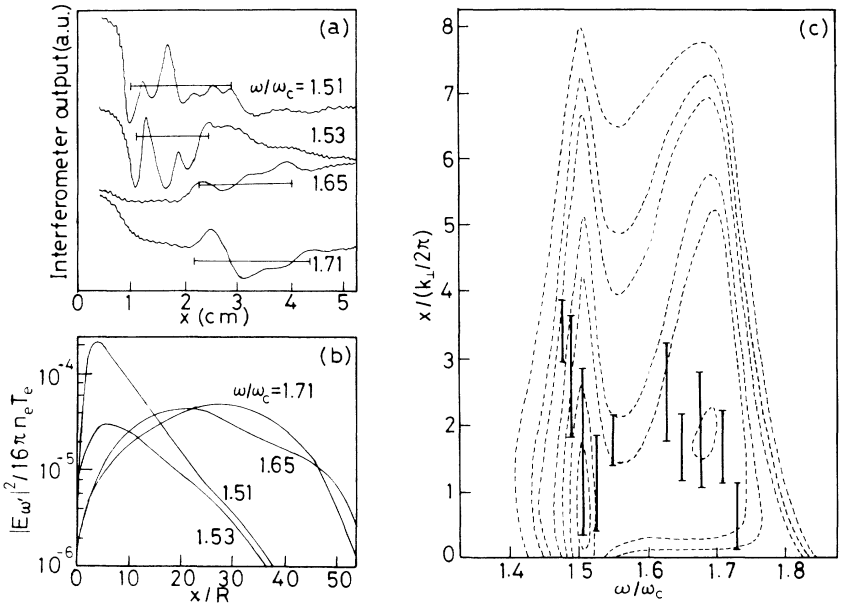

FIG. 3. (a) Interferometer output across the magnetic field for the wave $(\omega',\mathbf{k}')$. (b) Calculated spatial evolution of the field energy density of the virtual wave. (c) Vertical bars show locations of the detectable region of the wave $(\omega',\mathbf{k}')$, and dotted lines are the calculated equifield contour map of the virtual wave on the x-ω plane, where the lines are, from the outside, $|E_{\omega'}|^2/16\pi n_e T_e = 10^{-7}, 5\times10^{-7}, 10^{-6}, 5\times10^{-6}, 10^{-5}, 5\times10^{-5}, 10^{-4}$; $\omega_{p0}^2/\omega_c^2 = 9.0$, $|E_\omega|^2/16\pi n_e T_e = 0.0004$.

that these results contribute to the understanding of the ion-Bernstein-wave heating at half-harmonic ion cyclotron frequency, and the electron cyclotron harmonic wave heating, in a tokamak plasma.

The author wishes to thank Dr. R. Sugaya for suggesting the general scheme of calculations and Professor T. Dodo for discussion. Numerical calculations were made at the Computation Center of Kyushu, Ehime University, and the Institute of Plasma Physics, Nagoya University.

[1]M. Ono, G. A. Wurden, and K. L. Wong, Phys. Rev. Lett. **52**, 37 (1984).

[2]M. Ono *et al.*, Phys. Rev. Lett. **54**, 2339 (1985).

[3]K. Toi *et al.*, in *Proceedings of Tenth International Conference on Plasma Physics and Controlled Nuclear Fusion Research, London, 1984* (International Atomic Energy Agency, Vienna, 1985), Vol. 1, p. 523.

[4]H. Abe *et al.*, Phys. Rev. Lett. **53**, 1153 (1984).

[5]M. Porkolab, Phys. Rev. Lett. **54**, 434 (1985).

[6]R. Sugaya, Phys. Fluids **30**, 1730 (1987).

[7]R. E. Aamodt and W. E. Drummond, Phys. Fluids **7**, 1816 (1964).

[8]M. N. Rosenbluth, B. Coppi, and R. N. Sudan, Ann. Phys. (N.Y.) **55**, 248 (1969).

[9]M. Porkolab and R. P. H. Chang, Phys. Fluids **15**, 283 (1972).

[10]R. P. H. Chang and M. Porkolab, Phys. Fluids **15**, 297 (1972).

[11]R. Sugaya, Phys. Fluids **26**, 2693 (1983).

[12]M. Sugawa and R. Sugaya, J. Phys. Soc. Jpn. **54**, 1339 (1985).